Proceedings of the 1999 IEEE/RSJ
International Conference on
Intelligent Robots and Systems

Decoupled Dynamics and Stabilization of Single Wheel Robot

Kwok Wai Au and Yangsheng Xu
Department of Mechanical and Automation Engineering,
The Chinese University of Hong Kong, Hong Kong

Abstract

Gyrover is a single wheel, gyroscopically stabilized robot. It is a single wheel connected to a spinning flywheel through a two-link manipulator at the wheel bearing. The nature of the system is nonholonomic, nonlinear and underactuated. In this paper, we first develop a dynamic model and decouple the model with respect to the control inputs. We then study the effect of the flywheel dynamics on stabilizing the single wheel robot via simulation and experiment study. Finally, we design a linear state feekback control law that stabilizes the single wheel robot toward/in different lean angles, so as to control the precession rate. Simulation and experiment study validated the proposed controller as well as the developed dynamic model.

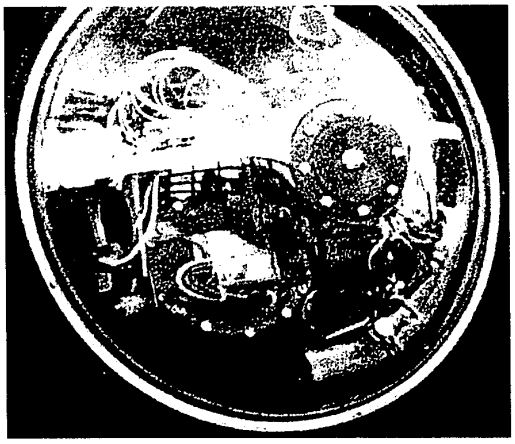

Figure 1: Photograph of the third prototype of Gyrover.

1 Introduction

Gyrover is a novel, single wheel gyroscopically stabilized robot, originally developed at Carnegie Mellon Universty [1]. Three prototypes have already been developed and tested; Figure 1 shows a photograph of the third prototype we developed recently. Essentially, Gyrover is a sharp-edged wheel, with an actuation mechanism fitted inside the wheel. The actuation mechanism consists of three different actuators: (1) *a spin motor* which spins a suspended flywheel at a high rate, imparting dynamic stability to the robot, (2) *a title motor* which controls the steering of Gyrover, and (3) *a drive motor* which produces the forward and/or backward acceration, by driving Gyrover directly.

The behavior of Gyrover is based on the principle of gyroscopic precession as exhibited in stability of a rolling wheel. Because of its angular momentum, a spinning wheel tends to precess at right angles to an applied torque, according to the fundamental equation of gyroscopic precession:

$$T = J \times \omega \times \Omega \qquad (1)$$

where ω is the angular speed of the wheel, Ω is the wheel's precession rate around the axis, normal to the spin axis, J is the wheel polar moment of inertia about the spin axis, and T is the applied torque, normal to the spin and precession axes. Therefore, when a rolling wheel leans to one side, instead of falling over, the gravitationally induced torque causes the wheel to precess so that it turns in the direction that it is leaning. Gyrover supplements this basic concept with the addition of an internal gyroscope, i.e., the spinning flywheel, nominally aligned with the wheel and spinning in the direction of forward motion. The flywheel's angular momentum produces lateral stability even if the robot moves in a low speed.

There has been some work on the dynamics and control of autonomous unicycles and bicycles. Schoonwinkel presented the work on an autonomous stabilized unicycle in [7] where he modeled the human-unicycle system as a three-bodies system, i.e., a wheel, a frame and a rotary turntable. In his model, he separated the lateral and longitudinal dynamics by perturbating the yaw rate to specific quantities. Vos and

0-7803-5184-3/99/$10.00 © 1999 IEEE

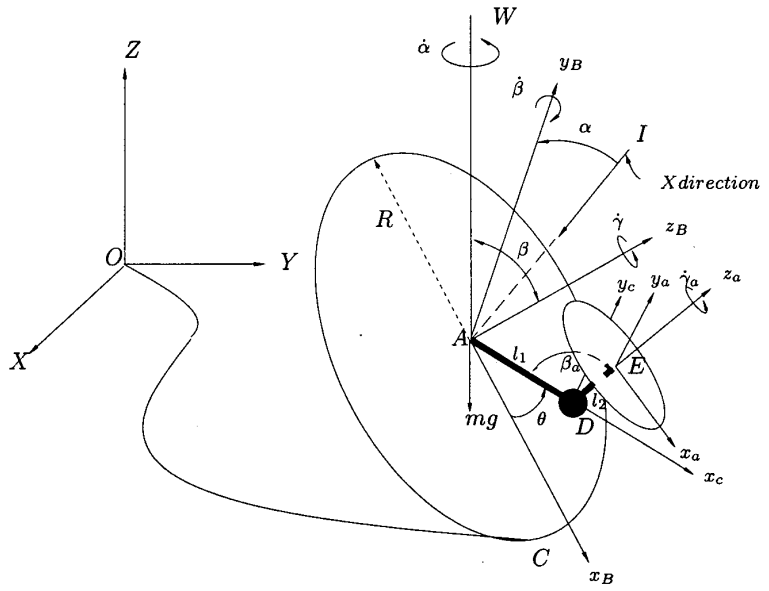

Figure 2: Definition of system variables for Gyrover

Flotow [8] based on the model of Schoonwinkel, developed a unicycle and implemented the LQG controller. Nakajima and others [4] designed a unicycle which is similar to a rugby ball where there is a rotary actuator between the upper and lower body in order to stabilize lateral dynamics and steering. They also decoupled the lateral and longitudinal motion. Beznos and others [5] studied gyroscopically stabilizied bicycle consisting of two coupled gyroscopes spinning in the opposite directions. They presented a linear model of the bicycle and the control law to track the motion along a straight line as well as a curve. Due to the gyroscopic stabilization, they assumed that the bicycle can always keep around the vertical position during the motion.

Most of the above mentioned work simplified the models by decoupling the yaw and roll dynamics. The single wheel robot is, however, different from the above mentioned system, in that the single wheel robot steers by leaning to different roll angles, based on the change of tilt angle of the flywheel. Therefore, the roll and yaw dynamics are highly coupled. In order to stabilize the single wheel robot and track the specific trajectory, we must understand this highly coupled dynamics so as to design a controller dealing with both yaw and roll dynamics simultaneously.

In our previous work [2] and [3], we developed a dynamic model using the constrained generalized Lagrangian formulation, with five independent generalized coordinates $\alpha, \beta, \gamma, \beta_a, \theta$ and two nonholonomic velocity constraints. In this paper, we first simplfied this model by considering the center of the flywheel coincident with the center of the single wheel robot. We decouple the tilting varible β_a from dynamic equation and consider $\dot{\beta}_a$ as a new input of the system, such that the number of the generalized coordinates and the dimension of the inertial matrix are reduced. Then, we studied the effect of the high spinning flywheel to the lateral stability of the robot, through the simulations and experiments. Based on linearization, the motion control is decomposed into three parts: (1) controlling the rolling speed $\dot{\gamma}$, (2) controlling the tilting variable $\beta_a(t)$ to the desired trajectory, and (3) designing a linear state feedback controller in order to control the lean angle β, so as to track specified trajectories such as a circle and a straight line.

2 Decoupled Dynamic Model

We developed the nonholonomic constraints and dynamic model of Gyrover in [3]. In derivation of the equations of motion, we assumed that the wheel is a rigid, homogeneous, disk which rolls over a perfectly flat surface without slipping. We model the actuation mechanism suspended from the wheel bearing, as a two-link manipulator, with a spinning disk attached at the end of the second link (Figure 2). The system

Table 1: Variable definition

α	Precession angles of the wheel
β	Lean angles of the wheel
β_a	tilt angle between the link l_1 and z_a-axis of the flywheel
γ, γ_a	Spin angles of the wheel and flywheel respectively
θ	Angle between link l_1 and x_B-axis of the wheel
m_w, m_i, m_f	Mass of the wheel, internal mechanism and flywheel respectively
m	Total mass of the robot
R, r	Radius of the wheel and the flywheel respectively
g	Gravitational acceleration
u_1, u_2	Drive torque for the dive motor and tilt torque for the tilt motor respectively
I_{xw}, I_{yw}, I_{zw}	Moment of inertia of the wheel about x, y and z axes
I_{xf}, I_{yf}, I_{zf}	Moment of inertia of the flywheel about x, y and z axes
μ_s, μ_g	Friction coefficient in yaw and pitch directions respectively
Ω_o, Ω	Nominal component and the small perturbation of the wheel angular velocity respectively
δ_β	Small perturbation of the lean angle around vertical position
δ_{β_a}	Small perturbation of the tilt angle around vertical position

parameters and varibles are shown in Table 1. For simplicity, l_1 and l_2 are assumed to be zero, thus the mass center of the flywheel coincides with the center of the robot. The pendulum motion of the internal mechanism is sufficiently small to be neglected, so that θ can be set to zero. The spinning rate of the flywheel γ_a is considered to be fixed.

Let $S_x := sin(x)$, $C_x := cos(x)$, $S_{\beta,\beta_a} := sin(\beta + \beta_a)$, $C_{\beta,\beta_a} := cos(\beta+\beta_a)$, and $S_{2\beta\beta_a} := sin[2(\beta+\beta_a)]$. Based on the derivation in [3], the *normal form*[1] of the dynamics model is

$$M(q)\ddot{q} = F(q, \dot{q}) + Bu \tag{2}$$

$$\dot{X} = R(\dot{\gamma}C_\alpha + \dot{\alpha}C_\alpha C_\beta - \dot{\beta}S_\alpha S_\beta) \tag{3}$$

$$\dot{Y} = R(\dot{\gamma}S_\alpha + \dot{\alpha}C_\beta S_\alpha + \dot{\beta}C_\alpha S_\beta) \tag{4}$$

where $q = [\alpha, \beta, \gamma, \beta_a]^T$,

$$M = \begin{bmatrix} M_{11} & 0 & M_{13} & 0 \\ 0 & I_{xf} + I_{xw} + mR^2 & 0 & I_{xf} \\ M_{13} & 0 & 2I_{xw} + mR^2 & 0 \\ 0 & I_{xf} & 0 & I_{xf} \end{bmatrix},$$

$$F = [F_1, F_2, F_3, F_4]^T,$$

$$B = \begin{bmatrix} 0 & 0 & 1 & 0 \\ 0 & 0 & 0 & 1 \end{bmatrix}^T, u = \begin{bmatrix} u1 \\ u2 \end{bmatrix}$$

$$M_{11} = I_{xf} + I_{xw} + I_{xw}C_\beta^2 + mR^2C_\beta^2 + I_{xf}C_{\beta,\beta_a}^2$$

$$M_{13} = 2I_{xw}C_\beta + mR^2C_\beta$$

[1]It is a reduced form of nonholonomic system by eliminating the constraint multipliers. One of procedure was introduced in [9].

$$F_1 = (I_{xw} + mR^2)S_{2\beta}\dot{\alpha}\dot{\beta} + I_{xf}S_{2\beta\beta_a}\dot{\alpha}\dot{\beta} + I_{xf}S_{2\beta\beta_a}\dot{\alpha}\dot{\beta}_a + 2I_{xw}S_\beta\dot{\beta}\dot{\gamma} + 2I_{xf}S_{\beta,\beta_a}\dot{\beta}\dot{\gamma}_a + 2I_{xf}S_{\beta,\beta_a}\dot{\beta}_a\dot{\gamma}_a$$

$$F_2 = -gmRC_\beta - (I_{xw} + mR^2)C_\beta S_\beta\dot{\alpha}^2 - I_{xf}C_{\beta,\beta_a}S_{\beta,\beta_a}\dot{\alpha}^2 - (2I_{xw} + mR^2)S_\beta\dot{\alpha}\dot{\gamma} - 2I_{xf}S_{\beta,\beta_a}\dot{\alpha}\dot{\gamma}_a$$

$$F_3 = 2(I_{xw} + mR^2)S_\beta\dot{\alpha}\dot{\beta}$$

$$F_4 = -I_{xf}C_{\beta,\beta_a}S_{\beta,\beta_a}\dot{\alpha}^2 - 2I_{xf}S_{\beta,\beta_a}\dot{\alpha}\dot{\gamma}_a$$

where (X, Y, Z) is the coordinates of center of mass of the robot with respect to the inertial frame as shown in Figure 2. $M(q) \in R^{4\times4}$ and $N(q, \dot{q}) \in R^{4\times1}$ are the inertial matrix and nonlinear term, respectively. Eq. (2) and Eqs. (3) and (4) form the dynamics model and nonholonomic velocity constraints of the robot.

We further simplify our model by decoupling the tilting variable β_a from Eq. (2). Practically, β_a is directly controlled by the tilt motor (position control), i.e., assuming that the tilt actuator has an adequate torque to track the desired $\beta_a(t)$ trajectory exactly. Therefore, β_a can be decoupled from Eq. (2). It is similar to the case of decoupling the steering variable from the bicycle dynamics shown in [5] and [6].

We consider $\dot{\beta}_a$ as a new input u_{β_a}, consequently the dynamics model Eq. (2) becomes

$$\begin{aligned} \dot{\beta}_a &= u_{\beta_a} \\ \tilde{M}(\tilde{q})\ddot{\tilde{q}} &= \tilde{F}(\tilde{q}, \dot{\tilde{q}}) + \tilde{B}\tilde{u}. \end{aligned} \tag{5}$$

with $\tilde{q} = [\alpha, \beta, \gamma]^T$,

$$\tilde{M} = \begin{bmatrix} M_{11} & 0 & M_{13} \\ 0 & I_{xf} + I_{xw} + mR^2 & 0 \\ M_{13} & 0 & 2I_{xw} + mR^2 \end{bmatrix}$$

$$\tilde{F} = \left[\tilde{F}_1, \tilde{F}_2, \tilde{F}_3\right]^T$$

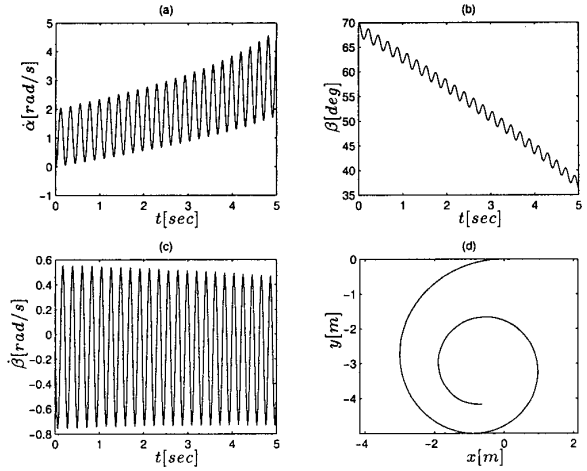

Figure 3: The simulation results of a rolling disk without flywheel.

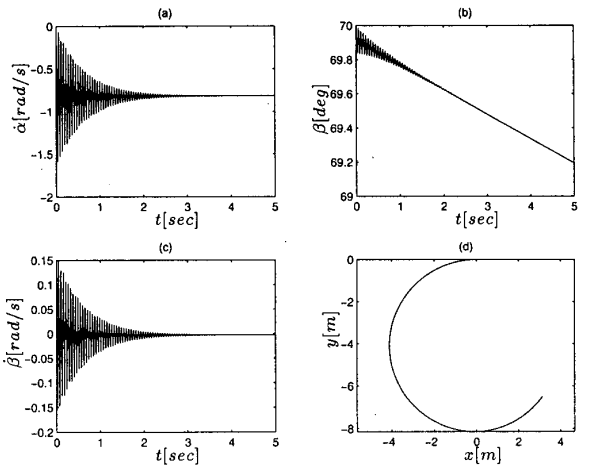

Figure 4: The simulation results of the single wheel robot.

$$\tilde{B} = \begin{bmatrix} 0 & 0 & 1 \\ \tilde{B}_{12} & 0 & 0 \end{bmatrix}^T, \tilde{u} = \begin{bmatrix} u_1 \\ u_{\beta_a} \end{bmatrix}$$

$$\begin{aligned} \tilde{F}_1 &= (I_{xw} + mR^2)S_{2\beta}\dot{\alpha}\dot{\beta} + I_{xf}S_{2\beta\beta_a}\dot{\alpha}\dot{\beta} - \dot{\alpha}\mu_\alpha \\ &\quad -2I_{xw}S_\beta\dot{\beta}\dot{\gamma} + 2I_{xf}S_{\beta,\beta_a}\dot{\beta}\dot{\gamma}_a, \\ \tilde{F}_2 &= F_2, \\ \tilde{F}_3 &= F_3, \\ \tilde{B}_{12} &= I_{xf}S_{2\beta\beta_a}\dot{\alpha} + 2I_{xf}S_{\beta,\beta_a}\dot{\gamma}_a, \end{aligned}$$

Eq. (5) shows the reduced dynamic model of the single wheel robot after decoupling the tilting varible β_a, with new matrices $\tilde{M}(\tilde{q}) \in R^{3\times3}$ and $\tilde{F}(\tilde{q}, \dot{\tilde{q}}) \in R^{3\times1}$. It is noted that if the lean angle β is set to be 90°, i.e., the single wheel robot falls on the ground, its inertial matrix $\tilde{M}$ becomes singular, because it violates the assumption of rolling without slipping.

3 Characteristics of the Robot Dynamics

The dynamics of the single wheel robot is highly coupled, nonholonomic and underactuacted. Its main component is a rolling wheel, therefore it processes the typical characteristics of a rolling disk. For a rolling disk, it will not fall when it is rolling because the gyroscopic torque, resulting from the coupling motion between the roll and yaw motions, balances the gravitational torque. However, its rolling rate must be large enough to provide a sufficient gyroscopic torque for balancing the disk. For the single wheel robot, its gyroscopic torque is greater, and less depends on its rolling speed $\dot{\gamma}$, owing to the high spinning flywheel. Thus, the lean angle of the robot will tend to remain unchanged. We can explain this characteristics based on the equilibrium solution of Eq. (5). For the low yaw rate and $\ddot{\alpha} = \ddot{\beta} = \ddot{\gamma} = 0, \dot{\beta} = 0, u_1 = u_{\beta_a} = 0$, Eq. (5) becomes

$$0 = gmRC_\beta + (2I_{xw} + mR^2)S_\beta\dot{\alpha}\dot{\gamma} + 2I_{xf}S_{\beta,\beta_a}\dot{\alpha}\dot{\gamma}_a, \quad (6)$$

From Eq. (6), the terms $\dot{\gamma}\dot{\alpha}$ and $\dot{\gamma}_a\dot{\alpha}$ are used to cancel the gravitational torques $gmRC_\beta$, in order to stabilize the roll component of the system. Because the spinning rate $\dot{\gamma}_a$ is very high, the term $2I_{xf}S_{\beta,\beta_a}\dot{\alpha}\dot{\gamma}_a$ is significantly large, in order to cancel the gravitational torque, even though the rolling speed $\dot{\gamma}$ is low. Thus, it will achieve an equilibrium steering rate $\dot{\alpha}_s$,

$$\dot{\alpha}_s = \frac{-gmRC_{\beta_s}}{2I_{xf}S_{\beta_s,\beta_a}\dot{\gamma}_a + (2I_{xw} + mR^2)S_{\beta_s}\dot{\gamma}} \quad (7)$$

for a specific lean angle β_s.

Figures 3 and 4 showed the simulation results of a rolling disk without the flywheel and the single wheel robot respectively, under the identical initial conditions

$$\begin{cases} \beta = 70°, \beta_a = 0°, \\ \dot{\beta} = \dot{\alpha} = \dot{\beta}_a = 0\ rad/s, \dot{\gamma} = 15\ rad/s, \\ \alpha = 0°. \end{cases}$$

Note that the lean angle β of a rolling disk without flywheel decreases much rapidly than that of the single wheel robot as shown in Figures 3(b) and 4(b).

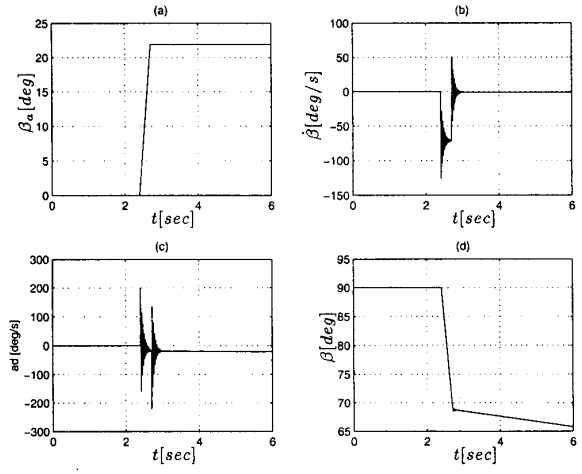

Figure 5: The simulation results of tilting the flywheel of the robot with $\dot{\beta}_a = 73\ deg/s$

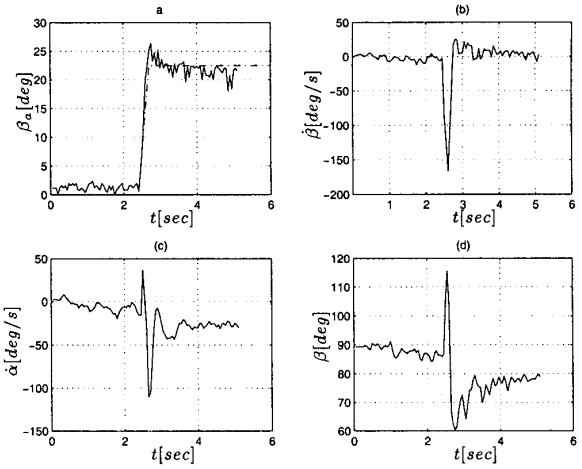

Figure 6: The experiment results of tilting the flywheel of the robot with $\dot{\beta}_a = 73\ deg/s$

This verifies the stabilizing effect of the flywheel to the robot. In Figures 4(a),(c), under the influence of friction in the yaw direction, the steering rate $\dot{\alpha}$ and the leaning rate $\dot{\beta}$ will converge to a steady state solution as shown in Eq. (7). Otherwise, the unwanted high frequency oscillation will occur. Practically, it will not produce a significant effect on the system because the frequency of the oscillation is much higher than the system dynamics. If the rolling rate is reduced, the rolling disk will fall much quickly than it is in the previous case.

Until now, we only consider the case when the flywheel's orientation is fixed with respect to the wheel. Here, we focus on the tilting effect of the flywheel to the robot. Based on conservation of the angular momemtum, when the tilt angle of the flywheel β_a changes, the whole robot will rotate in the *opposite direction* in order to maintain a constant angular momentum. It implies that we may control the lean angle of the robot for steering. Simulation and experiment results are shown in Figure 5 and Figure 6, respectively, under the initial condition

$$\begin{cases} \beta = 90^o, \beta_a = \alpha = 0^o, \\ \dot{\beta} = \dot{\alpha} = \dot{\beta}_a = 0\ rad/s, \dot{\gamma} = 15\ rad/s, \\ \alpha = 0^o. \end{cases}$$

Both Figures 5 and 6 show that if the tilt angle β_a rotates in 73 deg/sec counterclockwise at t = 2.4 second, the lean angle β rotates in clockwise direction . In the experiment, the transient response of β is more critical than the simulations. In 2.7 second, the tilt angle remains unchange and then β and steering rate $\dot{\alpha}$ converge to a steady position in both simulations and experiments. In the experiment, we have not found any high frequency oscillations, perhaps because the sensor response and the specified sampling time are set such that the high frequency oscillations are not shown.

4 Stabilization of Robot

We derive a linear model based on the following assumption: the spinning rate $\dot{\gamma}_a$ is sufficiently high so that the terms $\dot{\gamma}_a\dot{\beta}, \dot{\gamma}_a\dot{\alpha}$ are much greater than the terms $\dot{\beta}\dot{\gamma}, \dot{\beta}\dot{\alpha}, \dot{\alpha}^2$. We then linearize the system Eq. (5) around the vertical position with $\beta = 90^o + \delta_\beta, \dot{\gamma} = \Omega_o + \Omega, \beta_a = \delta_{\beta_a}$, as shown in Figure 7. The variable definitions are shown in Table 1. It can be expressed as

$$\begin{aligned} (I_{xf} + I_{xw})\ddot{\alpha} &= 2(I_{xw}\Omega_o + I_{xf}\dot{\gamma}_a)\dot{\delta}_\beta - \mu_s \\ &\quad +2I_{xf}\dot{\gamma}_a u_{\beta_a} \qquad (8) \\ (I_{xw} + mR^2)\ddot{\delta}_\beta &= gmR\delta_\beta - (2I_{xw} + mR^2)\Omega_o\dot{\alpha} \\ &\quad -2Ixf\dot{\gamma}_a\dot{\alpha} \qquad (9) \\ (2I_{xw} + mR^2)\dot{\Omega} &= -\mu_g\Omega + u_1 \qquad (10) \end{aligned}$$

Because Ω is independent of the roll and yaw dynamics Eq. (8) and Eq. (9), we can decompose the pitch dynamics Eq. (10) and set up a close loop for controlling the angular velocity of the single wheel robot Ω. The remaining yaw and roll dynamics form a state

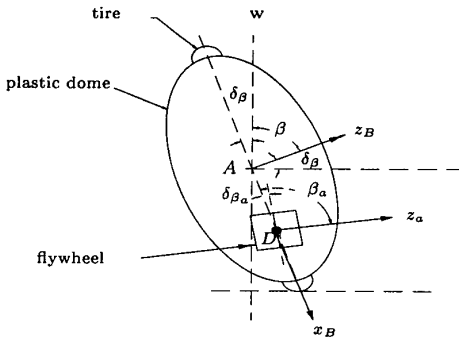

Figure 7: The lateral description of Gyrover.

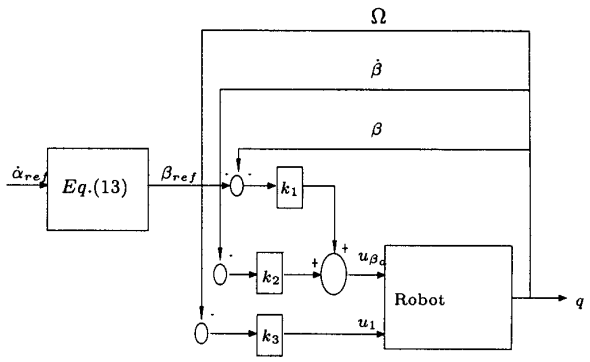

Figure 8: Schematic of the control algorithms.

equation shown below,

$$\dot{x} = Ax + Gu, \tag{11}$$

where $x = \left[\delta_\beta, \dot{\alpha}, \dot{\delta}_\beta\right]^T$,

$$A = \begin{bmatrix} 0 & 0 & 1 \\ 0 & a_{22} & a_{23} \\ a_{31} & a_{32} & 0 \end{bmatrix}, G = \begin{bmatrix} 0 \\ b_2 \\ 0 \end{bmatrix}$$

where $a_{22}, ..., a_{32}$ and b_2 are derived from Eqs. (8) and (9). Based on the controllability matrix, the system is controllable if $\dot{\gamma}_a \neq 0$ and $\dot{\gamma} \neq 0$. It is because if the single wheel robot is not rolling, it falls immediately. The system can be stabilized by using a linear state feedback

$$u_{\beta_a} = -k_1(\delta_\beta - \delta_{\beta ref}) - k_2\dot{\delta}_\beta - k_3(\dot{\alpha} - \dot{\alpha}_{ref}). \tag{12}$$

where k_1, k_2, k_3 are feedback gains, $\delta_{\beta ref}$ are the desired lean angle,

$$\dot{\alpha}_{ref} = \frac{gmR\delta_{\beta ref}}{(2I_{xw} + mR^2)\Omega_o + 2I_{xf}\dot{\gamma}_a} \tag{13}$$

In order to ensure an asymptotic stability of the system Eq. (11), the necessary conditions of the feedback gain are

$$k_1 < 0, k_2 < 0, k_3 > 0.$$

It ensures that all eignvalues of the closed loop system have negative real parts. The third control loop is used to track the desired $\beta_a(t)$ to provide the suitable u_{β_a} for the closed loop system Eq. (11).

In order to achieve the path following, it is desirable to control the forward speed and steering rate. From Eq. (10), we can control the forward speed by controlling the rolling speed of the robot (Ω). However, for the control of the steering rate, it exhibits nonminimum phase behaviour. If we consider the steering rate $\dot{\alpha}$ as the output of Eq. (11), the transfer function becomes

$$\begin{aligned} H(s) &= c(sI - A)^{-1}G \\ &= \frac{b_2(-a_{31} + s^2)}{s^3 - a_{22}s^2 - (a_{31} + a_{23}a_{32})s + a_{22}a_{31}} \end{aligned} \tag{14}$$

where $c = [0, 1, 0]$. From Eq. (14), there is a zero of $H(s)$ on the right-half plane, resulting in nonminimum phase. In order to track a desired steering rate $\dot{\alpha}_{ref}$, we track a roll angle β_{ref} that is compatible with $\dot{\alpha}_{ref}$ based on Eq. (13). We set up a closed loop control for tracking β_{ref} based on Eq. (12) as shown in Figure 8.

In the first simulation, we stabilized the robot at the vertical position ($\beta = 90°, \delta_{\beta ref} = 0°$), such that it moves in a straight line. The simulation results are shown in Figure 9. The initial conidtions are,

$$\begin{cases} \delta_\beta = 10°, \beta_a = \alpha = 0°, \\ \dot{\delta}_\beta = \dot{\alpha} = \dot{\beta}_a = 0\ rad/s, \dot{\gamma} = 15\ rad/s, \\ k_1 = -15, k_2 = -1, k_3 = 3 \end{cases}$$

From Figure 9, it shows that the lean angle β exponentially converge to 90°, so that the steering rate will exponentially converge to zero. Therefore the trajectory of the center of the robot was slightly curved at the beginning and then finally converged to a straight line.

Then we set $\delta_{\beta ref} = 20°$ and the simulation results are shown in Figure 10. Note that as $\delta_{\beta ref}$ was not eqaul to zero, there was a steady steering rate $\dot{\alpha}_{ref}$ according to the Eq. (13). As a result, its trajectory was a circle. The initial experiment has also verified the above result and will be demonstrated at the time of the conference.

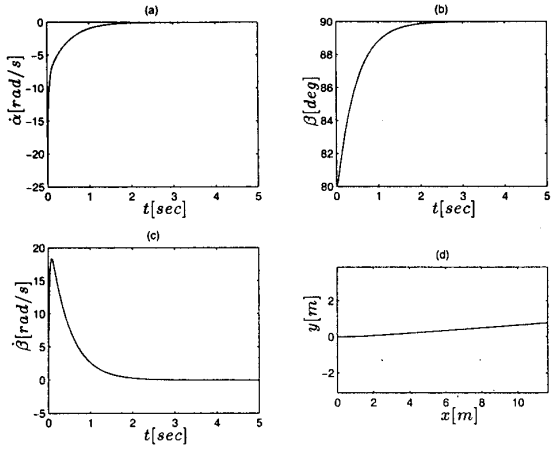

Figure 9: The simulation results of the single wheel robot stabilized to vertical position.

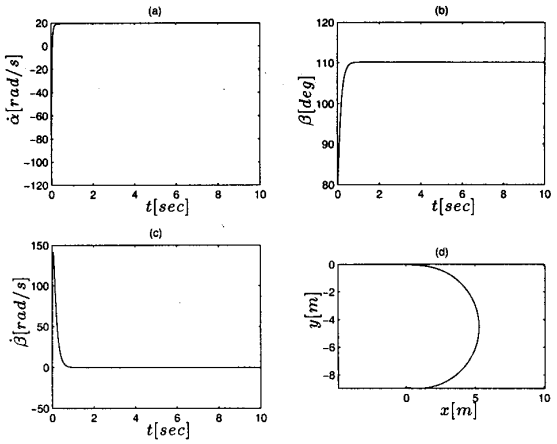

Figure 10: The simulation results of the single wheel stabilized to lean angle $\beta = 100°$.

5 Conclusion

In this paper, we simplified the dynamic model of the single wheel robot by decoupling the tilting variable from the original dynamics. The model was verified through the simulations and experiments. The lean angle of the robot can be directly controlled by tilting the flywheel, in order to achieve steering. We designed a linear state feedback to stabilize the robot to the desired lean angle, so as to control the steering rate of the robot. The work is significant in understanding the dynamics of the highly coupled and nonholonomic system, and is valuable in developing automatic control for the dynamically stable robot.

References

[1] H. B. Brown and Y. Xu., "A single wheel gyroscopically stabilized robot." *Proc. IEEE Int. Conf. on Robotic and Automation,* Vol. 4, pp. 3658-63, 1996.

[2] G. C. Nandy and Y. Xu, "Dynamic model of a gyroscopic wheel," *Proc. IEEE Int. Conf. on Robotic and Automation,* Vol. 3, pp. 2683-2688, 1998.

[3] Y. Xu, K. W. Au, G. C. Nandy and H. B. Ben, "Analysis of actuation and the dynamic balancing for a single wheel robot" *Proc. IEEE/RSJ Int. Conf. on Intelligent Robots and Systems,* Vol. 4, pp. 3658-63, 1998.

[4] R. Nakajima, T. Tsubouchi, S. Yuta and E. Koyanagi, "A development of a new mechanism of an autonomous unicycle," *Proc. IEEE/RSJ Int. Conf. on Intelligent Robots and Systems,* Vol. 4, pp. 3658-63, 1997.

[5] A. V. Beznos, A. M. Formal'sky, E. V. Gurfinkel, D. N. Jicharev, A. V. Lensky, K. V. Savitsky, L.S. Tchesalin "Control of autonomous motion of two-wheel bicycle with gyroscopic stabilisation" *Proc. IEEE Int. Conf. on Robotic and Automation,* Vol. 3, pp. 2670-2675, 1998.

[6] N. H. Getz, "Control of balance for a nonlinear nonholonomic non-minimum phase model of a bicycle" *Proc. ACC Conference, Baltimore, MD, June 1994,* 148-151.

[7] A. Schoonwinkel, "Design and test of a computer stabilized unicycle," Ph.D. dissertation, Stanford Univ., CA, 1987.

[8] D. W. Vos and A. H. von Flotow, "Dynamics and nonlinear adaptive control of an autonomous unicycle(theory and experiment)," *Proc. of the 29th IEEE Conf. on Decision and Control,* Vol. 3, pp. 2670-2675, 1998.

[9] Bloch, A. M., M. Reyhanoglu and N. H. McClamroch, "Control and stabilization of nonholonomic systems," *IEEE Trans. Aut. Control, vol. 37,* pp.1746-1757, 1992.